Proc. Indian Acad. Sci. (Chem. Sci.), Vol. 106, No. 2, April 1994, pp. 393–405.

Origin of the insulating state in $NaCuO_2$

SEVA NIMKAR[1,2], N SHANTHI[1] and D D SARMA[1,3]*

[1] Solid State and Structural Chemistry Unit,
[2] Department of Physics, and
[3] Jawaharlal Nehru Centre for Advanced Scientific Research, Indian Institute of Science, Bangalore 560012, India

Abstract. We study the electronic structure of $NaCuO_2$ by analysing experimental core level photoemission and X-ray absorption spectra using a cluster as well as an Anderson impurity Hamiltonian *including* the band structure of the oxygen sublattice. We show that the X-ray absorption results unambiguously establish a negative value of the charge transfer energy, Δ. Further, mean-field calculations for the edge-shared one-dimensional CuO_2 lattice of $NaCuO_2$ within the multiband Hubbard Hamiltonian show that the origin of the insulating nature lies in the band structure rather than in the correlation effects. LMTO–ASA band structure calculations suggest that $NaCuO_2$ is an insulator with a gap of around 1 eV.

Keywords. Origin of the insulating state; $NaCuO_2$ electronic structure; LMTO-band structure.

1. Introduction

The electronic structure of transition metal compounds in general and oxides in particular have traditionally been explained over the last decade in terms of the Zaanen–Sawatzky–Allen (ZSA) (1985, 1986a) phase diagram. It is now understood that both U_{dd} and Δ need to be larger than some critical values in order to obtain an insulating state in these strongly correlated systems. These conditions are often fulfilled for a large variety of $3d$ transition metal compounds, explaining the preponderance of such insulating compounds. However, recently Mizokawa *et al* (1991) analysed the photoemission, (PE) data of sodium copper oxide, $NaCuO_2$, using the cluster model and obtained a negative Δ value. This suggests that $NaCuO_2$ should be metallic in terms of the above mentioned phase diagram, since the ground state will correspond to the occupancy of the continuum states derived from the oxygen $2p$ band. On the contrary $NaCuO_2$ is an insulator with a bandgap of 1–2 eV. On the basis of these unusual observations, these authors suggested (Mizokawa *et al* 1991) that the ground state of $NaCuO_2$ may represent a new type of insulating state, attributing it to the existence of 90° Cu–O–Cu interaction in this compound leading to a narrow split-off localized state essentially with $d^9 L^1$ character. While their analysis of the electron spectroscopic results was carried out within the cluster model, these authors indicate that an impurity calculation with small or negative Δ value also yields a bandgap in accordance with their conclusions. It should be noted here

*For correspondence

that the possibility of formation of an insulating state due to strong interaction between metal *d* and oxygen *p* splitting off a continuum state was already shown a few years ago within the impurity model (Sarma and Taraphder 1989; Sarma 1990). In fact, even in the lattice limit the presence of such an insulating state with small Δ corresponding to the presence of a hole in the ligand levels, in the limit of the vanishing transfer integral, has been discussed by Sarma *et al* (1992); this has been termed the covalent insulator. However the covalent insulator phase was found for the position of the *d* level within the oxygen *p*-bandwidth (and thus, corresponding to an $\Delta_{eff} < 0$), but not for negative Δ-values (within the parameter range investigated by Sarma *et al* (1992), since the conventional measure of Δ is with respect to the oxygen *p*-band centre. Moreover it should be noted that the phase diagram calculated by Sarma *et al* (1992) modelled copper in its 2+ valence state (corresponding to La_2CuO_4) containing only one hole in the *d* band per copper ion, whereas copper is in the Cu^{3+} state in $NaCuO_2$ with 2 holes in the *d* band. As will be shown in this paper, the two-dimensional lattice corresponding to that of La_2CuO_4, but with copper in the 3+ valence state does lead to the formation of negative Δ covalent insulators. Hence, the negative Δ value of $NaCuO_2$ does not by itself imply a new kind of an insulating phase. It should also be noted here that the crystal structure of $NaCuO_2$ is such that it essentially contains one-dimensional chains of edge-shared CuO_2 units with 90° Cu–O–Cu interaction (Hestermann and Hoppe 1969) in contrast to the corner-shared CuO_2 units with 180° Cu–O–Cu interaction of the La_2CuO_4 lattice. This structural difference may in principle give rise to a different insulating phase; thus the problem clearly deserves a detailed analysis including the structural details. Such details could not possibly have been included in the earlier treatment (Mizokawa *et al* 1991) due to the limitation of the model. In the present work we have analysed the core level PE data (Mizokawa *et al* 1991) as well as the X-ray absorption (XA) data (Sarma *et al* 1988) of $NaCuO_2$ using the Anderson impurity Hamiltonian in contrast to the cluster model employed by earlier workers (Mizokawa *et al* 1991). Moreover, following our earlier work (Sarma and Taraphder 1989) we use the explicitly calculated oxygen 2*p* band states for the impurity calculations so as to account for the important structural information rather than assuming it to be semielliptical as is usually done (Zaanen *et al* 1986; Mizokawa *et al* 1991). Our analysis shows that though a wide range of Δ-values (*both negative and positive*) is compatible with the core level PE spectrum, the combined analysis of core level PE and XA spectra clearly indicates a negative Δ-value for $NaCuO_2$, in agreement with the earlier result (Mizokawa *et al* 1991) based on PE data alone. In order to understand the insulating property of $NaCuO_2$, however, it is important to go beyond the single impurity calculation and consider the lattice of Cu^{3+} to account for the bandwidths associated with Cu 3*d* states. Since the ensuing multiband Hubbard model cannot be solved exactly, we obtain the mean-field solution to this model including the spiral spin density wave (SDW) in an analogous way to our earlier work (Sarma *et al* 1992). Comparing the result obtained from the simplest lattice relevant for the $NaCuO_2$ crystal structure with a few other related lattices, we analyse the origin of the insulating phase of $NaCuO_2$ for negative Δ values. We find that the two-dimensional lattice with 180° Cu–O–Cu interaction with two holes in the *d* band does show the insulating phase for a moderately negative Δ. However we find that the one-dimensional lattice with 90° Cu–O–Cu interaction supports an insulator at very pronounced negative Δ values,

entirely due to band structure effects, where correlation effects do not play any qualitative role. A part of the results discussed here has been briefly presented in an earlier work (Nimkar *et al* 1993). In this context, we also point out the recent work of Karlsson *et al* (1992) who have discussed the core level lineshape as well as chemical shift of the core level in $NaCuO_2$ in contrast to mono- and divalent oxides of copper.

It should be noted here that the above analysis based on parametrized Hamiltonians depends crucially on the choice of the strengths of the various electronic interactions. Though attempts have been made here to obtain reliable estimates of these parameter strengths from an analysis of experimental spectroscopic data, the approach remains open to various pitfalls. For example, such approaches never represent an all-electron calculation; most importantly, only one copper d-orbital is included in the model many-body Hamiltonian for the sake of simplicity. Thus it cannot be ascertained if the gap or the insulating nature would survive inclusion of all the five d-orbitals. Here it is to be noted that the predicted origin of the insulating behaviour of $NaCuO_2$ is essentially single-particle in nature, being independent of the various Coulomb interactions. Thus, we have carried out band structure calculation of $NaCuO_2$ within the linear-muffin-tin orbital (LMTO) method to further strengthen our interpretations.

2. Methods of calculations

In order to compare our results with those of Mizokawa *et al* (1991) we first perform cluster calculations for the PE core level and the XA spectra. Within this approximation, we only retain the nearly square planar CuO_4 cluster appearing in $NaCuO_2$, idealised in our calculation to have the D_{4h} point group symmetry. We assume that the splitting between the $d_{x^2-y^2}$ and d_{z^2} is large enough to ensure an $S=0$ ground state. This is in conformity with the calculations of Mizokawa *et al* (1991) for $NaCuO_2$ and the doped hole case of La_2CuO_4 (Sarma and Ovchinnikov 1990); in both these cases a low-spin $^1A_1$ state is found to be the ground state. Since $NaCuO_2$ has a formal d^8 electron (or d^2 hole) configuration, we used $|d^2\rangle, |d^1p^1\rangle$ and $|p^2\rangle$ (in the hole configuration) as basis for the cluster calculations where $|d^2\rangle$ corresponds to two holes in the $d_{x^2-y^2}$ state; $|d^1p^1\rangle$ one hole each in the d_{x^2-y2} and b_{1g} symmetry-adapted oxygen p state; and $|p^2\rangle$ two holes in the symmetry-adapted oxygen p state. The Hamiltonian for the CuO_4 cluster with Cu $3d_{x^2-y^2}$ and b_{1g} symmetry adapted p-function as given by

$$H = (\varepsilon_d + U_{dc}n_c)n_d + \varepsilon_p n_p + U_{dd}n_{d\uparrow}n_{d\downarrow} + ta_d^\dagger a_p + \text{h.c.},$$

where ε_p and ε_d are the bare on-site energies of the oxygen $2p$ and copper $3d$ orbitals respectively, U_{dd} is the on-site Coulomb repulsion for the d holes, U_{dc} is the Coulomb repulsion between the d and core holes and t is the transfer integral between the $d_{x^2-y^2}$ and the b_{1g} symmetry-adapted oxygen p state. $t = 3^{1/2}t_{pd\sigma}$, $t_{pd\sigma}$ being the usual Slater–Koster (1954) integral. n_d and n_p are the number operators for the copper d and oxygen p orbitals respectively; $a_d^\dagger$ creates a d hole and a_p annihilates a p hole. Here $n_c = 0$ corresponds to the initial state of the photoemission process with no core hole and $n_c = 1$ represents the final state with a core hole. The relevant matrix elements

to calculate the PE spectrum are

$$\langle d^2|H|d^2\rangle = 0,$$
$$\langle d^2|H|d^1p^1\rangle = 2^{1/2}t,$$
$$\langle d^1p^1|H|d^1p^1\rangle = \Delta - U_{dc}n_c,$$
$$\langle d^1p^1|H|p^2\rangle = 2^{1/2}t,$$
$$\langle p^2|H|p^2\rangle = 2\Delta - 2U_{dc}n_c + U_{dd},$$

where $\Delta(=\varepsilon_p\varepsilon d - U_{dd})$ is the bare charge transfer energy. For the XA spectrum the initial state is the same as that used in the PE calculation (i.e. $n_c = 0$). The final state has a core hole and one less hole in the valence states as the XA process transfers an electron from the core to the valence levels and the Hamiltonian matrix is then defined with respect to two basis vectors $|d^1\rangle$ and $|p^1\rangle$. We calculate the spectra from the above models in the usual way (Sarma and Taraphder 1989; Sarma and Ovchinnikov 1990; Mizokawa *et al* 1991) assuming the sudden approximation, and obtain the parameter range for Δ, t, U_{dd} and U_{dc} which provides a good fit to the experimental data of the photoemission and X-ray absorption spectra.

In order to go beyond the limitations of the cluster model by taking into account the band structure of the oxygen sublattice in a realistic way, we have performed calculations within the Anderson impurity Hamiltonian with the copper atom as an impurity embedded in the oxygen sublattice. The crystal structure of $NaCuO_2$ clearly shows the existence of one-dimensional arrays of edge-shared CuO_2 units, with a large separation ($\sim 2{\cdot}87$ Å) between two such chains (Hestermann and Hoppe 1969). Thus we consider the arrangement of oxygen in this lattice as one-dimensional edge-shared square units with two oxygen atoms per unit cell. We include only the oxygen $2p_x$ and $2p_y$ in-plane orbitals, ignoring the $2p_z$ orbitals. The resulting tight-binding bands are given by

$$\varepsilon_k^{1,2} = \varepsilon_p - 2t_{pp\sigma}\cos(kx) \mp t_{pp\pi},$$
$$\varepsilon_k^{3,4} = \varepsilon_p - 2t_{pp\pi}\cos(kx) \pm t_{pp\sigma},$$

where $t_{pp\sigma}$, $t_{pp\pi}$ are the usual Slater–Koster (1954) integrals. Throughout our calculations, we have assumed $t_{pp\sigma}$ and $t_{pp\pi}$ to be 0·7 and $-0{\cdot}3$ eV, respectively. The impurity Hamiltonian in this approximation is given by

$$H = \sum_{ik\sigma} \varepsilon_k^i n_{ik\sigma} + \sum_{\sigma} (\varepsilon_d + U_{dc}n_c)n_{d\sigma} + \sum_{ik\sigma} (V_{kd}^i a_{d\sigma}^\dagger a_{ik\sigma} + \text{h.c.}) + U_{dd}n_{d\uparrow}n_{d\downarrow}, \quad (1)$$

where $a_{d\sigma}^\dagger$ creates a d hole with spin σ and $a_{ik\sigma}$ annihilates a ligand hole with momentum $\mathbf{k}$ and spin σ. ε_k^i are the oxygen band energies ($i = 1$ to 4), ε_d is the single d-hole energy and the U's are as defined before. The charge transfer energy, $\Delta(= E(d^1\,L^1) - E(d^2))$, is measured with respect to the middle of the oxygen **p**-band and is given by $\Delta = \varepsilon_p - \varepsilon_d - U_{dd}$. The hybridization matrix elements V_{kd}^i are the hopping interaction strengths between the copper $d_{x^2-y^2}$ orbital and the oxygen p band i.e. $V_{kd}^i = \langle\psi^i(k,r)|H|d(r=0)\rangle$ with $i = 1$ to 4, where $\psi^i(k,r)$ are the oxygen band eigenfunctions. It turns out that there is no hopping interaction between the copper $d_{x^2-y^2}$

and the first as well as the third oxygen bands and

$$V_{kd}^2 = -(3/2)^{1/2} t_{pd\sigma}(1 + e^{ikx}),$$
$$V_{kd}^4 = (3/2)^{1/2} t_{pd\sigma}(1 - e^{ikx}),$$

where $t_{pd\sigma}$ is the Slater–Koster integral. The problem of solving the Hamiltonian in (1) can be considerably simplified using the transformation (Bringer and Lustfeld 1977; Gunnarsson and Schönhammer 1978, 1983)

$$|V(\varepsilon)|^2 = \sum_{i,k} |V_{kd}^i|^2 \delta(\varepsilon - \varepsilon_k^i)$$

and rewriting the Hamiltonian as

$$H = \sum_{i\sigma} \varepsilon_i n_{i\sigma} + \sum_{\sigma} (\varepsilon_d + U_{dc} n_c) n_{d\sigma} + \sum_{i\sigma} (V(\varepsilon_i) a_{d\sigma}^\dagger a_{i\sigma} + \text{h.c.}) + U_{dd} n_{d\uparrow} n_{d\downarrow}. \quad (2)$$

Here the continuum band states have been discretized by the N levels with energies ε_i, $i = 1$ to N. On the basis of this Hamiltonian, (2), Gunnarsson and Schönhammer (1978, 1983) showed that various high-energy spectroscopic results can be calculated for a wide range of systems. It appears that use of a small number of discretized states to represent the bands provides fairly well-converged results. In practice, N as small as 6 has been used (Kotani *et al* 1985). We have used $N = 10$ in the present calculations. As mentioned for the cluster calculation we work in $S = 0$ subspace with the basis $|d^2\rangle (= |d_\uparrow^1 d_\downarrow^1\rangle)$, $|d^1\, L^1\rangle (= 1/2^{1/2}(|d_\uparrow^1\, L_\downarrow^1\rangle + |d_\downarrow^1\, L_\uparrow^1\rangle)$, $|L_i^1\, L_j^1\rangle (= 1/2^{1/2}$ $(|L_{i\uparrow}^1\, L_{j\downarrow}^1\rangle + |L_{i\downarrow}^1\, L_{j\uparrow}^1\rangle)$ for $i \neq j$ and $|L^2\rangle (= |L_{i\uparrow}^1\, L_{i\downarrow}^1\rangle)$. The photoemission core level spectra were calculated using the following matrix elements

$$\langle d^2|H|d^2\rangle = 0$$
$$\langle d^2|H|d^1\, L_i^1\rangle = 2^{1/2}\, V(\varepsilon_i),$$
$$\langle d^1\, L_i^1|H|d^1\, L_j^1\rangle = (\Delta - \varepsilon_p - U_{dc} n_c + \varepsilon_i)\delta_{ij},$$
$$\langle d^1\, L_i^1|H|\, L_i^1\, L_i^1\rangle = 2^{1/2}\, V(\varepsilon_i),$$
$$\langle L_i^1\, L_j^1|H|\, L_i^1\, L_j^1\rangle = \varepsilon_i + \varepsilon_j,$$
$$\langle d^1\, L_k^1|H|L_i^1\, L_j^1\rangle = V(\varepsilon_i)\delta_{kj} + V(\varepsilon_j)\delta_{ki} \quad \text{for} \quad i \neq j.$$

The initial ($n_c = 0$) Hamiltonian matrix elements are the same for the XA calculation. The final state Hamiltonian matrix elements for the XA calculation are written using the basis $|d^1\rangle$ and $|L_i^1\rangle$, as it involves only one hole in the valence orbitals. Once again, as in the cluster calculations, the calculated spectrum is made to fit the experimental spectrum by varying the parameters Δ, t, U_{dd} and U_{dc}.

In order to understand the existence of an insulating phase in the negative Δ regime, it is *absolutely essential* to go beyond the impurity Hamiltonian, as the impurity split-off state would have an associated band-width due to inter-cluster interactions. Thus we used the Hubbard–Hamiltonian for the one-dimensional chain of edge-sharing CuO_2 unit cells within a Hartree–Fock approximation (HFA) allowing for spiral SDW (Sarma *et al* 1992). The Hamiltonian is

$$H = \sum_{i\sigma} \varepsilon_d d_{i\sigma}^\dagger \mathrm{d}_{i\sigma} + \sum_{i\sigma\gamma} \varepsilon_p (a_{\gamma i\sigma}^\dagger a_{\gamma i\sigma} + b_{\gamma i\sigma}^\dagger b_{\gamma i\sigma})$$

$$+\sum_{\langle ij\rangle\sigma} t^{ij}_{pp\sigma}\left(\sum_{\gamma} a^{\dagger}_{\gamma i\sigma}a_{\gamma j\sigma}+b^{\dagger}_{1i\sigma}b_{2j\sigma}\right)+\sum_{\langle ij\rangle\sigma} t^{ij}_{pp\pi}\left(a^{\dagger}_{1i\sigma}a_{2j\sigma}+\sum_{\gamma} b^{\dagger}_{\gamma i\sigma}b_{\gamma j\sigma}\right)$$

$$+\sum_{\langle ij\rangle\sigma\gamma} t^{ij}(d^{\dagger}_{i\sigma}a_{\gamma j\sigma}+d^{\dagger}_{i\sigma}b_{\gamma j\sigma})+\text{h.c.}+U_{dd}\sum_{i} d^{\dagger}_{i\uparrow}d_{i\uparrow}\,d^{\dagger}_{i\downarrow}d_{i\downarrow}\,, \tag{1}$$

where $d^{\dagger}_{i\sigma}$, $a^{\dagger}_{1i\sigma}$, $a^{\dagger}_{2i\sigma}$, $b^{\dagger}_{1i\sigma}$ and $b^{\dagger}_{2i\sigma}$ for the ith unit cell corresponds to creating a hole with spin σ in the $d_{x^2-y^2}, p_x, p_y$ orbitals at site 1 and 2 with a and b denoting the two oxygen orbitals p_x and p_y in the unit cell. ε_d and ε_p are the bare hole energies; t^{ij}'s are the transfer integrals and U_{dd} is the on-site Coulomb repulsion for the d holes. We decouple the four fermion terms in the mean field approximation and use the ansatz

$$\langle S^{+}\rangle = |b_0|e^{i\mathbf{Q}\cdot\mathbf{r}_i}$$

to allow for the spiral SDW, where $\mathbf{Q}$ is the spiral wave vector.

The band structure of $NaCuO_2$ has been calculated in the linearized Muffin-tin orbital method with the atomic sphere approximation (ASA) (Anderson 1975; Skriver 1984). In the LMTO method, the potential in the solid is approximated by a spherically averaged potential within the muffin-tin sphere around each atom and the secular equations linearized in energy around a fixed energy E^{l}_{v} for each partial wave. An energy-independent basis set constructed from partial waves that are solutions inside the muffin-tin sphere is employed. In the ASA the space is divided in terms of spheres centred on each atom; the radii of the spheres are so chosen that the sum of the volumes of the spheres equals the unit cell volume. This is known as the space-filling criterion. In order to acheive this space-filling the spheres are made slightly overlapping. If the overlap of different spheres required in this process is unreasonably large empty spheres are introduced to satisfy space-filling with reasonable overlaps.

The triclinic unit cell (Hestermann and Hoppe 1969) of $NaCuO_2$ contains one formula unit. Nonrelativistic and spin-restricted calculations were carried out to self-consistency with the atomic sphere radii 3·2039 atomic units (a.u.) for Na, 2·5809 a.u. for Cu and 2·2765 a.u. for O. We used s, p, d basis for each atomic sphere. The calculation is performed with 216 k-points in the Brillouin zone for self-consistency. In the present calculation E_v's were chosen to be at the centre of gravity of the occupied part for each of the l-components. This procedure provides the best potential for the ground state properties. The density of states is obtained from the self-consistent potential with 512 k-points.

3. Results and discussion

The experimental core level PE spectrum (Mizokawa *et al* 1991) of $NaCuO_2$ is shown in figure 1. The spectrum shows a main peak with two satellites in the $2p_{3/2}$ energy region. The main peak at $\sim$932·7 eV has been assigned (Mizokawa *et al* 1991) primarily to $d^{10}\,L^2$ character whereas the two satellites at $\sim$941·5 and $\sim$953 eV have $d^9\,L^1$ and d^8 characters respectively. The d^8 related feature associated with the $2p_{3/2}$ photoemission process overlaps with the $d^{10}\,L^2$ satellite of the $2p_{1/2}$ energy region, making the estimate of the energy position and intensity of the d^8 satellite somewhat uncertain. We estimate the energy difference between $d^{10}\,L^2$ and d^8 features to be

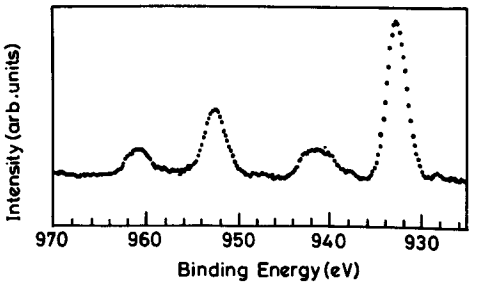

Figure 1. Experimental core level photoemission spectra from Mizokawa *et al* (1991).

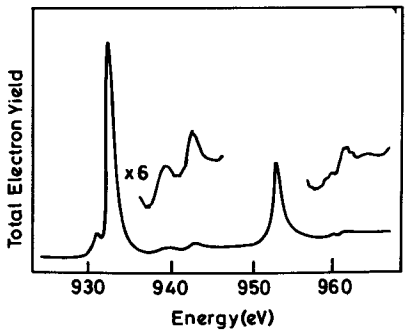

Figure 2. Experimental X-ray absorption spectra taken from Sarma *et al* (1988). The small intensity shoulder at about -2 eV is due to an impurity.

$\sim 20 \pm 2$ eV and the intensity of d^8 to be less than 20% of the total intensity. The $d^{10}L^2$ and d^9L^1 energy difference is $\sim 9 \pm 0{\cdot}5$ eV and their intensity ratio $I(d^{10}L^2)/I(d^9L^1)$ is $\sim 1{\cdot}3 \pm {\cdot}3$.

Figure 2 shows the XA spectrum obtained in Sarma *et al* (1988). Here the main peaks at ~ 933 and ~ 953 eV (corresponding to $2p_{3/2}$ and $2p_{1/2}$ energy regions) have primarily $d^{10}L^1$ character, while the absorption peaks at ~ 941 and ~ 944 eV ($2p_{3/2}$) and at ~ 953 eV ($2p_{1/2}$) arise from essentially d^9 final states. The energy difference is estimated to be $\sim 9{\cdot}0 \pm 0{\cdot}5$ eV and the intensity ratio, $I(d^9)/I(d^{10}L)$, is $\sim 0{\cdot}07 \pm 0{\cdot}03$. Having established estimates for the various intensity ratios and energy separations, we simulate the experimental spectra using the cluster model. In this we limit $|\Delta|$ to be less than 4 eV and t to lie between 2 and 3·5 eV based on the experience from other transition metal compounds. Also U_{dd} and U_{dc} were allowed to vary between the wide range of 5 and 15 eV. In figure 3a we show the valid range of Δ and t values that reproduces the experimental spectra of PE, while in figure 3b we show the combinations of Δ and t compatible with the XA spectrum. From figure 3a we see that both positive and negative Δ values are compatible with the PE data, whereas figure 3b clearly shows that only negative Δ values can describe the XA spectrum. Comparing figure 3a and b we also find a range of Δ, t values ($\Delta \sim -3$ to -4 eV and $t \sim 2{\cdot}2$ to 2·8 eV) which fits both the PE spectrum and the XA spectrum. However, if we restrict the U_{dc} values to be within the range $U_{dd} < U_{dc} < 1{\cdot}3\,U_{dd}$ as has often been done (Mizokawa *et al* 1991) we obtain a somewhat narrow range for the Δ and

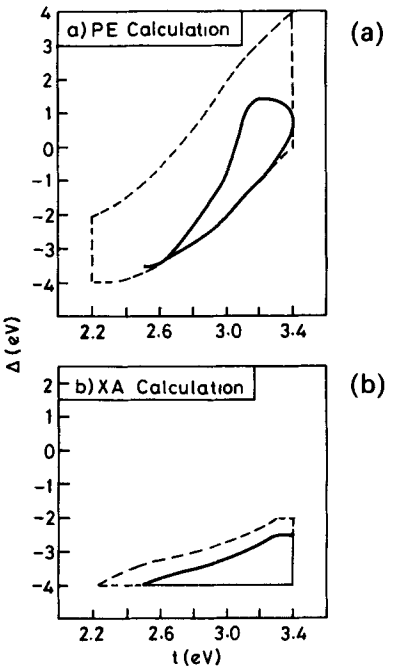

Figure 3. The enclosed region shows the range of parameter values of Δ and t obtained from a cluster calculation that is compatible with the experimental spectra. The smaller region inscribed by solid line is obtained when U_{dc} is constrained to be $U_{dd} < U_{dc} < 1{\cdot}3\ U_{dd}$ (see text), for (**a**) core level photoemission spectrum; (**b**) X-ray absorption spectrum.

t that describe the experimental spectra. The solid line in the figure enclose this range. Within this restricted range of U_{dc}, though the parameter values compatible with the XA and PE processes do not actually overlap, the two sets of solutions are found to be very close for Δ about $-3{\cdot}5$ eV and t about 2·6 eV. Keeping in mind the uncertainties in the energy and intensity ratios, we consider that these values give a reasonable description of the experimental spectra and compare well with those of (Mizokawa *et al* 1991) ($\Delta \sim -2 \pm 1$ eV and $t \sim 2{\cdot}7 \pm 0{\cdot}2$ eV).

Since it has been suggested (Mizokawa *et al* 1991) that the electronic structure of $NaCuO_2$ is unique due to the arrangement of the copper and oxygen atoms in the lattice that forms an essentially one-dimensional chain of edge-shared CuO_2 units with Cu–O–Cu 90° interactions, we decided to carry out the calculations within the impurity model as well, taking into account the band structure of the oxygen sublattice explicitly, as described in the previous section. Once again, we allow the parameters to vary as in the cluster calculation. Figure 4a and b show the Δ and t values that provide a reasonable fit to the experimental spectra of the PE and XA processes within the impurity approximation. Here too we see that both positive and negative Δ values reproduce the PE spectrum but only negative Δ values are compatible with the XA data. On imposing the condition $U_{dd} < U_{dc} < 1{\cdot}3U_{dd}$ as before, the Δ and t range is considerably narrowed, as shown by the region enclosed within the solid line in figure 4a and b. As in the cluster calculation we once again look for parameter values which are close to the range obtained from the PE and the XA spectra

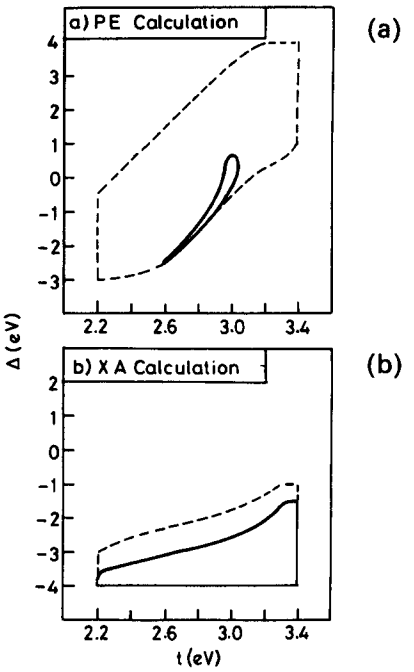

Figure 4. Parameter values of Δ and t obtained from an impurity calculation that is compatible with the experimental spectra are shown enclosed in dashed lines. The smaller region inscribed by solid line is obtained when U_{dc} is constrained to be $U_{dd} < U_{dc} < 1{\cdot}3\,U_{dd}$, for (**a**) core level photoemission spectrum; (**b**) X-ray absorption spectrum.

calculations and find that $\Delta \sim -2{\cdot}5$ eV and $t \sim 2{\cdot}6$ eV provide a good description for both the experimental spectra within this approximation. Here we see that the region of t is nearly the same as in the cluster calculation, but the Δ value is 1 eV larger compared to the ones obtained from cluster calculations. This is not surprising because the oxygen–oxygen hybridization t_{pp}, present in the impurity calculations but not included in the cluster calculations, lifts the degeneracy of the symmetry-adopted oxygen p orbitals. In particular, the energy of the b_{1g} symmetry adopted oxygen p function which interacts with the Cu $3d_{x^2-y^2}$ orbital, is shifted by $(t_{pp\sigma} - t_{pp\pi})$ with respect to the oxygen p-band centre (Sarma and Ovchinnikov 1990). With the values of $t_{pp\sigma}$ (= 0·7 eV) and $t_{pp\pi}$ (= −0·3 eV) used here, we thus obtain a shift of 1 eV of the relevant oxygen p states, explaining the shift in the Δ-value between the different approximations.

The parameter estimates above establish that $NaCuO_2$ has a negative Δ value. While the insulating state in $NaCuO_2$ may appear surprising in the presence of a negative Δ, the nature of the insulating state can be understood using a ZSA-like phase diagram, as shown below. An insulating state arising mainly from Cu d–O p hybridization has been discussed for the 180° Cu–O–Cu interaction in a 2-d CuO_2 lattice with one hole in the CuO_2 unit cell in an earlier work (Sarma *et al* 1992). These insulators were termed "covalent insulators". The effective-Δ was found to be negative for this state and the origin of the insulating state was due to strong pd hybridization. Since $NaCuO_2$ has two holes in the CuO_2 unit cell (i.e. Cu is in 3+

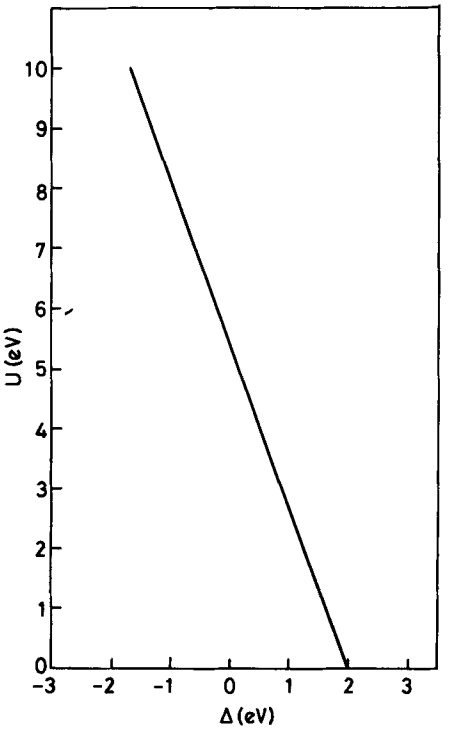

Figure 5. The phase line in $U_{dd} - \Delta$ plane, separating the metallic and insulating phases for the two-dimensional CuO_2 lattice.

valence state), we performed calculation similar to that done for Cu^{2+}. For these calculations the hybridization strengths relevant for $NaCuO_2$ were $t_{pp\sigma} = 0{\cdot}7\,eV$, $t_{pp\pi} = -0{\cdot}3\,eV$ and $t = 2{\cdot}6\,eV$ as obtained from the analysis presented above. The phase diagram thus obtained is shown in figure 5. It is to be noted that for $U > 6\,eV$, insulating states with negative Δ exist. This shows that negative Δ insulators are not unique to 90° Cu–O–Cu interactions. We studied the energy dispersion curves when $U_{dd} = 0$ and $\Delta = 2{\cdot}5\,eV$. The uppermost filled band has 70% *d* character and 30% *p* character. The lowest unoccupied band has predominantly (99%) *p* character. Hence the band gap is of *pd–p* kind. When $U_{dd} = 0$ the model reduces to a tight-binding model and the ground state is a band insulator. For $U_{dd} = 12\,eV$, $\Delta = -1\,eV$. The highest filled band has 58·5% *d* and 41·5% *p* character and the lowest unoccupied band has essentially only *p* character, making it once again *pd–p* bandgap.

The above computed phase diagram proves the existence of negative Δ insulators in general. However, $NaCuO_2$ has a one-dimensional chain of CuO_2 unit cells with 90° Cu–O–Cu interaction, while the above calculation of the phase diagram is for a two-dimensional lattice. In order to understand the consequences of this unique geometrical arrangement, a similar calculation, as for the La_2CuO_4 case, but with the $NaCuO_2$ structure and with the hybridization strengths as given before was performed. The metal–insulator phase line as a function of U_{dd} and Δ thus obtained is shown in figure 6. Note the large negative Δ values for which this structure with 90° Cu–O–Cu interaction supports insulating ground states. It is found that a band

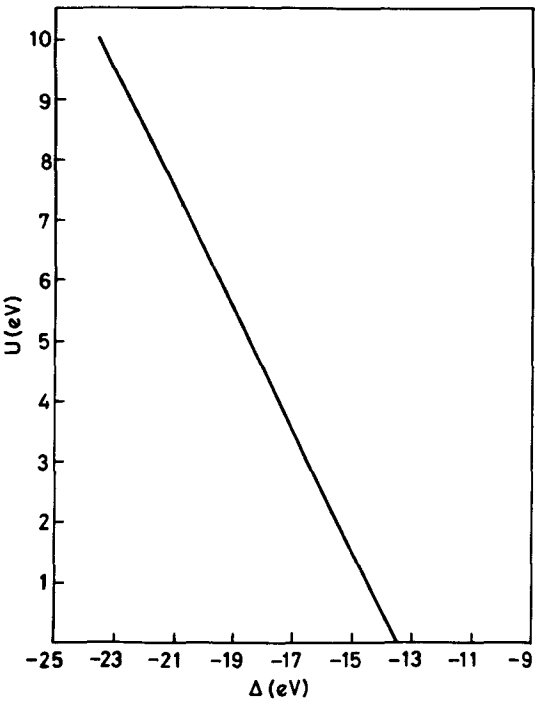

Figure 6. The metal–insulator phase diagram in $U_{dd} - \Delta$ plane for one-dimensional CuO_2 lattice with 90° Cu–O–Cu interactions.

insulator ground state exists for all Δ greater than -13 eV since the insulating state survives in the limit of $U_{dd} \to 0$. For $\Delta = -5$ eV and $U_{dd} = 0$, the highest filled band has 10·5% *d* and 89·5% *p* character and the lowest unoccupied band has essentially *p* character. Thus here we have a band insulator with the gap nearly of the *p–p* type. As in the band covalent insulator mentioned before, here too we obtain a zero gap for vanishing *t*. As we move away from the phase line by making Δ less negative, the band gap increases and the *d* character of the filled band increases changing the gap character continuously to a *pd–p* gap. This indicates that as the d^2 level is brought closer to the *p* band from above, the hybridization between copper *d* and oxygen *p* causes an increased *pd* character of the split-off state responsible for the opening up of the gap. For the parameters relevant for $NaCuO_2$ ($U_{dd} = 8$ eV and $\Delta = -2{\cdot}5$ eV) we find that the filled band has 47·5% *p* and 52·5% *d* character with the lowest unoccupied band having 99% *p* character. Thus it is a *pd–p* bandgap similar to the covalent insulator phase discussed earlier and not the *p–p* type gap as suggested by Mizokawa *et al* (1991). Nevertheless, it should still be kept in mind that (unlike for the CuO_2 planar structure) the underlying origin of the gap in the $NaCuO_2$ is still the band structure effects and the U_{dd}-value only increases the bandgap, but is not essential for the existence of the gap. In this sense, it is distinct from the Mott–Hubbard, charge-transfer and correlated covalent insulators which exist only in presence of finite U_{dd}. The origin of this bandgap in $NaCuO_2$ is thus predominantly single-particle (uncorrelated) in nature. While the bandgap in $NaCuO_2$ opens up due to covalency effects, it is interesting to note that even a small value of *t* is sufficient to

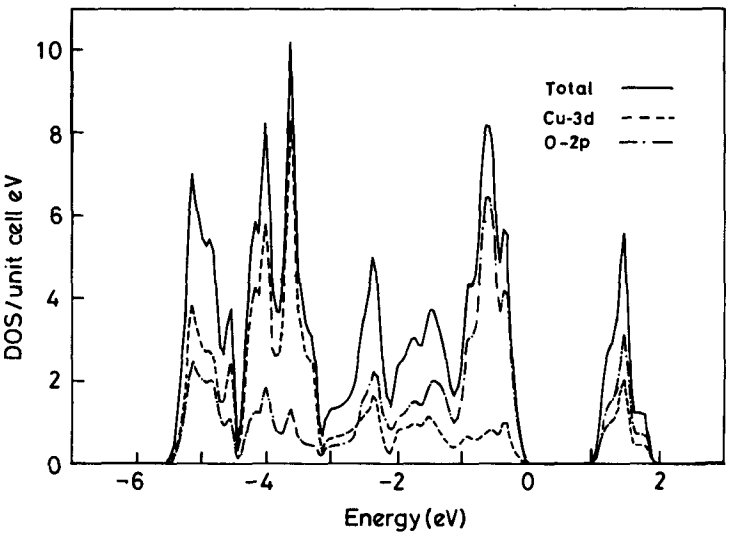

Figure 7. The total as well as partial Cu 3*d* and O 2*p* densities of states for $NaCuO_2$ obtained from LMTO–ASA calculations. The zero of the energy scale corresponds to the energy of the topmost occupied band.

sustain the bandgap down to very negative values of Δ; this originates from the specific geometric arrangements of the lattice including the one-dimensional chain of edge-shared nearly square-planar CuO_2 units with 90° Cu–O–Cu interaction.

The CuO_2 unit cell considered in the above model has D_{4h} symmetry. Hence the model included only one copper *d* orbital corresponding to the b_{1g} respresentation which is the only empty orbital for Cu in the 3 + state. Besides ignoring the other *d* orbitals the coupling of the different chains in the structure has been assumed to be negligible. Since our conclusions have attributed the insulating nature of $NaCuO_2$ to solely single particle effects and the geometric structure, the insulating ground state should be describable within band structure calculations. Thus we have performed a calculation of the density of states (DOS) for $NaCuO_2$ within the LMTO–ASA method. The resulting DOS is shown in figure 7. From this figure it is clear that the total density of states obtained from this calculation exhibits a bandgap of about 1 eV in good comparison with our model calculation.

In conclusion we have taken the structure of $NaCuO_2$ explicitly into account and studied the electronic structure of $NaCuO_2$. We have analysed the experimental core level photoemission and X-ray absorption spectra with those calculated within configuration interaction model for a cluster as well as in the impurity limit. While the photoemission core level spectrum is compatible with both positive and negative Δ values, the X-ray absorption results clearly establish a negative Δ for this compound. We have obtained the metal-insulator phase diagrams in the U_{dd} and Δ plane for two lattices, one with one-dimensional Cu–O–Cu 90° interaction relevant for $NaCuO_2$, another with two-dimensional Cu–O–Cu 180° interaction. Comparing these we show that the one-dimensional lattice supports the insulating phase even for very large negative Δ values and its origin is essentially due to single-particle band structure effects in contrast to insulating states driven essentially by correlation

effects. Band structure calculations using the linear-muffin-tin orbital method confirm our interpretation.

Acknowledgements

We thank the Council of Scientific and Industrial Research, New Delhi for support. We also thank Drs M Methfessel, A T Paxton and M van Schiljgaarde for making the LMTO–ASA program available to us and Dr S Krishnamurthy for the initial help in setting up the LMTO–ASA program.

References

Anderson O K 1975 *Phys. Rev.* **B12** 3060
Bringer A and Lustfeld H 1977 *Z. Phys.* **B28** 213
Gunnarsson O and Schönhammer K 1978 *Z. Phys.* **B30** 297
Gunnarsson O and Schönhammer K 1983 *Phys. Rev.* **B28** 4315
Hestermann K and Hoppe R 1969 *Z. Anorg. Allg. Chem.* **367** 267
Karlsson K, Gunnarsson O and Jepsen O 1992 *J. Phys. – Condensed Matter* **4** 895 2801
Kotani A, Mizuta H, Jo T and Parlebas J C 1985 *Solid State Commun* **53** 805
Mizokawa T, Namatame H, Fujimori A, Akeyama K, Kondoh H, Kuroda H and Kosugi N 1991 *Phys. Rev. Lett.* **67** 1638
Nimkar S, Sarma D D and Krishnamurthy H R 1993 *Phys. Rev.* **B47** 10927
Sarma D D 1990 *J. Solid State Chemi.* **88** 45
Sarma D D, Krishnamurthy H R, Nimkar S, Ramasesha S, Mitra P P and Ramakrishnan T V 1992 *Pramana (J. Phys.)* **38** L531
Sarma D D and Ovchinnikov S G 1990 *Phys. Rev.* **B42** 6817
Sarma D D, Strebel O, Simmons C T, Neukirch U, Kaindl G, Hoppe R and Müller H P 1988 *Phys. Rev.* **B37** 9784
Sarma D D and Taraphder A 1989 *Phys. Rev.* **B39** 11570
Skriver H L 1984 *The LMTO method* (Berlin: Springer–Verlag)
Slater J C and G F Koster 1954 *Phys. Rev.* **B94** 1498
Zaanen J, Sawatzky G A and Allen J W 1985 *Phys. Rev. Lett.* **55** 418
Zaanen J, Sawatzky G A and Allen J W 1986a *J. Magn. and Magn. Mater.* **54–57** 609
Zaanen J, Westra C and Sawatzky G A 1986 *Phys. Rev.* **B33** 8060